Scientific Research Publishing

International Journal of Astronomy and Astrophysics, 2022, 12, 177-193
https://www.scirp.org/journal/ijaa
ISSN Online: 2161-4725
ISSN Print: 2161-4717

New Probability Distributions in Astrophysics: VIII. The Truncated Weibull—Pareto Distribution

Lorenzo Zaninetti

Department of Physics, Turin, Italy
Email: l.zaninetti@alice.it

How to cite this paper: Zaninetti, L. (2022) New Probability Distributions in Astrophysics: VIII. The Truncated Weibull—Pareto Distribution. *International Journal of Astronomy and Astrophysics*, **12**, 177-193.
https://doi.org/10.4236/ijaa.2022.122011

Received: April 4, 2022
Accepted: June 7, 2022
Published: June 10, 2022

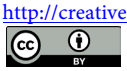

Abstract

We derive the truncated version of the Weibull—Pareto distribution, deriving the probability density function, the distribution function, the average value, the rth moment about the origin, the media, the random generation of values and the maximum likelihood estimator which allows deriving the three parameters. The astrophysical applications of the Weibull—Pareto distribution are the initial mass function for stars, the luminosity function for the galaxies of the Sloan Digital Sky Survey, the luminosity function for QSO and the photometric maximum of galaxies of the 2 MASS Redshift Survey.

Keywords

Stars: Normal, Galaxy Groups, Clusters, Superclusters, Large Scale Structure of the Universe, Cosmology

1. Introduction

Regarding probability distributions, in recent years there have been many modifications of the standard distributions: here we analyze the case of the Weibull distribution. The Weibull distribution has two parameters, the scale and the shape, see [1] [2] [3]. The new Weibull-Pareto distribution (NWPD) has three parameters: the scale and two shapes, see [4] [5] [6], and allows modelling the flooding of the Wheaton river and bladder cancer [5], provides a way to design a multiple deferred state acceptance sampling plans for assuring the lifetime of products [7], the stress-strength model [8] and the breaking stress of carbon fibers [9]. Some generalizations of the NWPD have been suggested [10] [11] [12]. One example of a probability distribution in astrophysics is the lognormal dis-

tribution for the initial mass function (IMF), which allows modelling 8 young clusters [13]. Another example is the Schechter luminosity function (LF) for galaxies [14], which is currently used to model the absolute magnitude in catalogs of galaxies such as the 2dF Galaxy Redshift Survey (2dFGRS) [15], the Sloan Digital Sky Survey (SDSS) [16] and the Millennium Galaxy Catalogue (MGC) [17]. The previous two arguments allow exploring old and new probability distributions in order to understand which produces the best fit. At the time of writing, the effect of a truncation on the NWPD has not yet been explored, and therefore, after a review in Section 2, its effect on the NWPD will be explored in Section 3. Section 4 is devoted to the derivation of the luminosity function for galaxies using both the regular and truncated versions, and then Section 5 is devoted to the astrophysical applications, such as the initial mass function for stars, the photometric maximum of the number of galaxies and the average absolute magnitude for galaxies.

2. The Weibull—Pareto Distribution

Let X be a random variable defined on $[0,\infty]$; the two-parameter *Weibull* distribution function (DF), $F_w(x)$, is

$$F_w(x;b,c)=1-\mathrm{e}^{-\left(\frac{x}{b}\right)^c}, \tag{1}$$

where b and c, both positive, are the scale and the shape parameters, see [18]. The NWPD is also defined on $[0,\infty]$:

$$F(x;a,b,c)=1-\mathrm{e}^{-a\left(\frac{x}{b}\right)^c}, \tag{2}$$

where a is a new positive shape parameter and the PDF, f, is

$$f(x;a,b,c)=\frac{a\left(\frac{x}{b}\right)^{c-1}c\mathrm{e}^{-a\left(\frac{x}{b}\right)^c}}{b}. \tag{3}$$

Careful attention should be paid to the fact that the transformation

$$b=b'a^{\frac{1}{c}}, \tag{4}$$

in Equation (2) followed by $b'=b$ transforms the NWPD DF into the Weibull DF.

The statistical parameters can be parametrized by introducing the following function

$$\Gamma_i=\Gamma\left(1+i/c\right), \tag{5}$$

where

$$\Gamma(z)=\int_0^\infty \mathrm{e}^{-t}t^{z-1}\mathrm{d}t, \tag{6}$$

is the gamma function, see [19].

The average value or mean, μ, is

$$\mu(a,b,c)=\frac{b\Gamma_0}{ca^{\frac{1}{c}}}, \tag{7}$$

the variance, σ^2, is

$$\sigma^2(a,b,c)=\frac{a^{-\frac{2}{c}}b^2\left(\Gamma_2c^2-\Gamma_0^2\right)}{c^2}, \tag{8}$$

the skewness is

$$\text{skewness}(a,b,c)=\frac{\Gamma_3c^3-3\Gamma_2\Gamma_0c^2+2\Gamma_0^3}{\left(\Gamma_2c^2-\Gamma_0^2\right)^{\frac{3}{2}}}, \tag{9}$$

and the kurtosis

$$\text{kurtosis}(a,b,c)=\frac{c^4\Gamma_4-4c^3\Gamma_0\Gamma_3+6\Gamma_0^2\Gamma_2c^2-3\Gamma_0^4}{\left(\Gamma_2c^2-\Gamma_0^2\right)^2}. \tag{10}$$

The rth moment about the origin for the NWPD, μ_r', is

$$\mu_r'(a,b,c)=\frac{b^r\Gamma\left(\frac{r}{c}\right)r}{ca^{\frac{r}{c}}}, \tag{11}$$

where r is an integer. The median is at

$$e^{\frac{\ln(\ln(2))-\ln(a)}{c}}b, \tag{12}$$

and the mode is at

$$\left(\frac{c-1}{ac}\right)^{\frac{1}{c}}b. \tag{13}$$

Random generation of the NWPD variate X is given by

$$X:a,b,c\approx\left(-\frac{\ln(1-R)}{a}\right)^{\frac{1}{c}}b \tag{14}$$

where R is the unit rectangular variate. One method to derive the three parameters a, b and c is to numerically solve the three following equations which arise from the maximum likelihood estimator (MLE)

$$\frac{n}{a}-\left(\sum_{i=1}^{n}\left(\frac{x_i}{b}\right)^c\right)=0, \tag{15a}$$

$$\frac{c\left(\left(\sum_{i=1}^{n}\left(\frac{x_i}{b}\right)^c\right)a-n\right)}{b}=0, \tag{15b}$$

$$-n\ln(b)+\frac{n}{c}+\sum_{i=1}^{n}\left(-a\left(\frac{x_i}{b}\right)^c\ln\left(\frac{x_i}{b}\right)+\ln(x_i)\right)=0, \tag{15c}$$

where the x_i are the elements of the experimental sample with i varying between 1 and n. Another method to derive the parameters is to introduce the moments of the experimental sample

$$\overline{x}_r = \frac{1}{n}\sum_i^n x_i^r . \tag{16}$$

The three parameters can then be found by solving the following three non-linear equations (the method of moments)

$$\overline{x}_1 = \mu_1'(a,b,c) = 0, \tag{17a}$$

$$\overline{x}_2 = \mu_2'(a,b,c) = 0, \tag{17b}$$

$$\overline{x}_3 = \mu_3'(a,b,c) = 0. \tag{17c}$$

Figure 1 reports the influence of the second shape parameter, a, of the NWPD on the Weibull distribution.

3. The Truncated Weibull—Pareto Distribution

The right and left truncated NWPD, see Equation (3), is defined on $[x_l, x_u]$ and has PDF

$$f_{DT}(x;a,b,c,x_l,x_u) = \frac{a x^{c-1} b^{-c} c \mathrm{e}^{-a x^c b^{-c}}}{-\mathrm{e}^{-a x_u^c b^{-c}} + \mathrm{e}^{-a x_u^c b^{-c}}}, \tag{18}$$

where a, b, c, x_l and x_u are positive parameters and DT means double truncation. The DF is

$$D_{DT}(x;a,b,c,x_l,x_u) = \frac{-\mathrm{e}^{-a x_u^c b^{-c}} + \mathrm{e}^{-a x^c b^{-c}}}{\mathrm{e}^{-a x_u^c b^{-c}} - \mathrm{e}^{-a x_u^c b^{-c}}}. \tag{19}$$

The average is

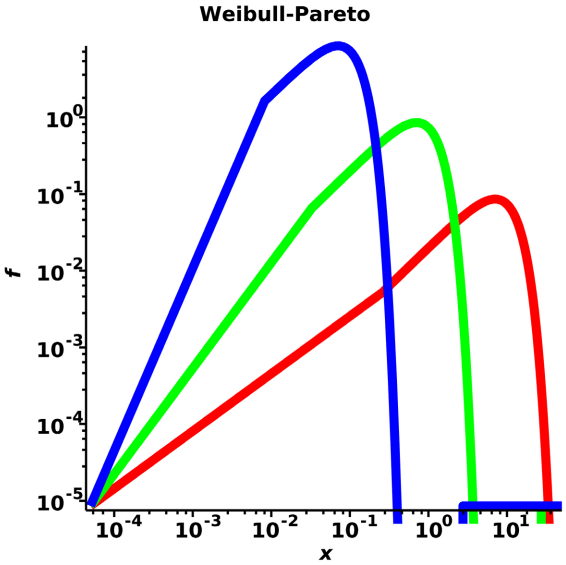

Figure 1. NWPD PDF with $b=1$, $c=2$ with $a=1/100$ (red line), with $a=1$ (green line) and with $a=100$ (blue line).

$$
\begin{aligned}
&\mu_{DT}\left(x;a,b,c,x_l,x_u\right)\\
&=\frac{1}{\left(\mathrm{e}^{-ax_u^c b^{-c}}-\mathrm{e}^{-ax_u^c b^{-c}}\right)(c+1)(2c+1)(3c+1)}\\
&\times\left(\left(4a^{-\frac{2c+1}{2c}}\mathrm{e}^{-\frac{ax_u^c b^{-c}}{2}}b^c\left(c+\frac{1}{2}\right)^2 x_u^{\frac{1}{2}-c}M_{\frac{2c+1}{2c},\frac{3c+1}{2c}}\left(ax_u^c b^{-c}\right)\right.\right.\\
&-4a^{-\frac{2c+1}{2c}}x_u^{\frac{1}{2}-c}\mathrm{e}^{-\frac{ax_u^c b^{-c}}{2}}b^c\left(c+\frac{1}{2}\right)^2 M_{\frac{2c+1}{2c},\frac{3c+1}{2c}}\left(ax_u^c b^{-c}\right)\\
&+\left(\mathrm{e}^{-\frac{ax_u^c b^{-c}}{2}}\left(2x_u^{\frac{1}{2}-c}b^c\left(c+\frac{1}{2}\right)a^{-\frac{2c+1}{2c}}+\sqrt{x_l}a^{-\frac{1}{2c}}c\right)M_{\frac{1}{2c},\frac{3c+1}{2c}}\left(ax_l^c b^{-c}\right)\right.\\
&\left.\left.\left.-M_{\frac{1}{2c},\frac{3c+1}{2c}}\left(ax_u^c b^{-c}\right)\left(2x_u^{\frac{1}{2}-c}b^c\left(c+\frac{1}{2}\right)a^{-\frac{2c+1}{2c}}+\sqrt{x_u}a^{-\frac{1}{2c}}c\right)\mathrm{e}^{-\frac{a x_u^c b^{-c}}{2}}\right)c\right)\sqrt{b}c\right),
\end{aligned}
\tag{20}
$$

where $M_{\mu,\nu}(z)$ is the Whittaker M function, see [19]. The variance exists but has a complicated expression. The rth moment about the origin for the truncated NWPD is

$$
\begin{aligned}
&\mu_r'\left(a,b,c,x_l,x_u\right)_{DT}\\
&=\frac{1}{(c+r)(2c+r)(3c+r)\left(-\mathrm{e}^{-ax_u^c b^{-c}}+\mathrm{e}^{-ax_l^c b^{-c}}\right)}\\
&\times\left(-\left(4x_l^{\frac{r}{2}-c}a^{-\frac{B}{2c}}\mathrm{e}^{-\frac{ax_l^c b^{-c}}{2}}b^{c+\frac{r}{2}}\left(c+\frac{r}{2}\right)^2 M_{1+\frac{r}{2c},\frac{3}{2}+\frac{r}{2c}}\left(ax_l^c b^{-c}\right)\right.\right.\\
&-4a^{-\frac{B}{2c}}x_u^{\frac{r}{2}-c}\mathrm{e}^{-\frac{ax_u^c b^{-c}}{2}}b^{c+\frac{r}{2}}\left(c+\frac{r}{2}\right)^2 M_{1+\frac{r}{2c},\frac{3}{2}+\frac{r}{2c}}\left(ax_u^c b^{-c}\right)\\
&+\left(\left(2x_l^{\frac{r}{2}-c}b^{c+\frac{r}{2}}\left(c+\frac{r}{2}\right)a^{-\frac{B}{2c}}+b^{\frac{r}{2}}x_l^{\frac{r}{2}}a^{-\frac{r}{2c}}c\right)\mathrm{e}^{-\frac{ax_l^c b^{-c}}{2}}M_{\frac{r}{2c},\frac{3}{2}+\frac{r}{2c}}\left(ax_l^c b^{-c}\right)\right.\\
&\left.\left.\left.-\mathrm{e}^{-\frac{ax_u^c b^{-c}}{2}}\left(2x_u^{\frac{r}{2}-c}b^{c+\frac{r}{2}}\left(c+\frac{r}{2}\right)a^{-\frac{B}{2c}}+b^{\frac{r}{2}}x_u^{\frac{r}{2}}a^{-\frac{r}{2c}}c\right)M_{\frac{r}{2c},\frac{3}{2}+\frac{r}{2c}}\left(ax_u^c b^{-c}\right)\right)c\right)c\right).
\end{aligned}
\tag{21}
$$

The median is at

$$
\mathrm{e}^{\frac{\ln\left(\ln(2)-\ln\left(\mathrm{e}^{-ax_l^c b^{-c}}+\mathrm{e}^{-ax_u^c b^{-c}}\right)\right)-\ln(a)+c\ln(b)}{c}},
\tag{22}
$$

and the mode is at the same value of the NWPD, see Equation (13). The random generation of the truncated NWPD variate X is given by

$$
X:a,b,c,x_l,x_u\approx b\left(-\frac{\ln\left(-R\mathrm{e}^{-ax_l^c b^{-c}}+R\mathrm{e}^{-a x_u^c b^{-c}}+\mathrm{e}^{-ax_l^c b^{-c}}\right)}{a}\right)^{\frac{1}{c}}.
\tag{23}
$$

The two parameters x_l and x_u are here assumed to be the minimum and the maximum of the experimental sample. The remaining three parameters, a, b and

c, can be determined by numerically solving the three following equations which arise from the MLE

$$\frac{1}{\left(-\mathrm{e}^{-ax_u^c b^{-c}}+\mathrm{e}^{-ax_l^c b^{-c}}\right)a}\left(b^{-c}x_l^c\mathrm{e}^{-ax_l^c b^{-c}}an-b^{-c}\mathrm{e}^{-ax_u^c b^{-c}}x_u^c an\right.$$
$$\left.-b^{-c}\mathrm{e}^{-ax_l^c b^{-c}}\left(\sum_{i=1}^{n}x_i^c\right)a+b^{-c}\mathrm{e}^{-ax_u^c b^{-c}}\left(\sum_{i=1}^{n}x_i^c\right)a+\mathrm{e}^{-ax_l^c b^{-c}}n-\mathrm{e}^{-ax_u^c b^{-c}}n\right)=0 \tag{24}$$

$$\frac{1}{b\left(-\mathrm{e}^{-ax_u^c b^{-c}}+\mathrm{e}^{-ax_l^c b^{-c}}\right)}\left(-\left(b^{-c}x_l^c\mathrm{e}^{-ax_l^c b^{-c}}an-b^{-c}\mathrm{e}^{-ax_u^c b^{-c}}x_u^c an\right.\right.$$
$$\left.\left.-b^{-c}\mathrm{e}^{-ax_l^c b^{-c}}\left(\sum_{i=1}^{n}x_i^c\right)a+b^{-c}\mathrm{e}^{-ax_u^c b^{-c}}\left(\sum_{i=1}^{n}x_i^c\right)a+\mathrm{e}^{-ax_l^c b^{-c}}n-\mathrm{e}^{-ax_u^c b^{-c}}n\right)c\right)=0 \tag{25}$$

$$\frac{1}{\left(-\mathrm{e}^{-ax_u^c b^{-c}}+\mathrm{e}^{-ax_l^c b^{-c}}\right)c}\left(-b^{-c}x_l^c\mathrm{e}^{-ax_l^c b^{-c}}\ln(b)acn+b^{-c}x_l^c\mathrm{e}^{-ax_l^c b^{-c}}\ln(x_l)acn\right.$$
$$+b^{-c}\mathrm{e}^{-ax_u^c b^{-c}}x_u^c\ln(b)acn-b^{-c}\mathrm{e}^{-ax_u^c b^{-c}}x_u^c\ln(x_u)acn-\mathrm{e}^{-ax_l^c b^{-c}}\ln(b)cn$$
$$+\mathrm{e}^{-ax_u^c b^{-c}}\ln(b)cn+c\left(\sum_{i=1}^{n}\left(ax_i^c\left(\ln(b)-\ln(x_i)\right)b^{-c}+\ln(x_i)\right)\right)\mathrm{e}^{-ax_l^c b^{-c}}$$
$$\left.-c\left(\sum_{i=1}^{n}\left(ax_i^c\left(\ln(b)-\ln(x_i)\right)b^{-c}+\ln(x_i)\right)\right)\mathrm{e}^{-ax_u^c b^{-c}}+\mathrm{e}^{-ax_l^c b^{-c}}n-\mathrm{e}^{-ax_u^c b^{-c}}n\right)=0 \tag{26}$$

where the x_i are the elements of the experimental sample with i varying between 1 and n.

4. Luminosity Function for Galaxies

In this section we derive the luminosity function for galaxies (LF) using both the regular and truncated DFs.

4.1. Using the Regular DF

In order to derive the NWPD LF, we start from the PDF as given by Equation (3),

$$\Psi\left(L;a,c,L^*,\Psi^*\right)\mathrm{d}L=\Psi^*\frac{a\left(\frac{L}{L^*}\right)^c c\mathrm{e}^{-a\left(\frac{L}{L^*}\right)^c}}{L}\mathrm{d}L, \tag{27}$$

where L is the luminosity defined for $[0,\infty]$, L^* is the characteristic luminosity and Ψ^* is a normalization, *i.e.* the number of galaxies in a cubic Mpc. We now introduce the following useful formulae relating the absolute magnitude and luminosity

$$\frac{L}{L_\odot}=10^{0.4(M_\odot-M)},\frac{L^*}{L_\odot}=10^{0.4\left(M_\odot-M^*\right)} \tag{28}$$

where $L_\odot$ and $M_\odot$ are the luminosity and absolute magnitude of the sun in the considered band. The LF in absolute magnitude is therefore

$$\Psi\left(M;a,c,M^*,\Psi^*\right)\mathrm{d}M=\Psi^*0.4a10^{\left(-0.4M+0.4M^*\right)c}c\mathrm{e}^{-a10^{\left(-0.4M+0.4M^*\right)c}}\ln\left(10\right)\mathrm{d}M. \quad (29)$$

4.2. Using the Truncated DF

The truncated NWPD LF for galaxies according to Equation (18) is

$$\Psi\left(L;a,c,L^*,\Psi^*,L_l,L_u\right)\mathrm{d}L=\Psi^*\frac{-a\left(\frac{L}{L^*}\right)^c c\mathrm{e}^{-a\left(\frac{L}{L^*}\right)^c}}{L\left(\mathrm{e}^{-a\left(\frac{L_u}{L^*}\right)^c}-\mathrm{e}^{-a\left(\frac{L_l}{L^*}\right)^c}\right)}\mathrm{d}L, \quad (30)$$

where the random variable L is defined for $\left[L_l,L_u\right]$, L_l is the lower boundary in luminosity, L_u is the upper boundary in luminosity, L^* is the characteristic luminosity and Ψ^* is the normalization. The magnitude version is

$$\begin{aligned}&\Psi\left(M;a,c,M^*,\Psi^*,M_l,M_u\right)\mathrm{d}M\\&=\Psi^*\frac{-0.4a\left(10^{0.4M^*-0.4M}\right)^c c\mathrm{e}^{-a\left(10^{0.4M^*-0.4M}\right)^c}\left(\ln\left(2\right)+\ln\left(5\right)\right)}{\mathrm{e}^{-a\left(10^{-0.4M_l+0.4M^*}\right)^c}-\mathrm{e}^{-a\left(10^{-0.4M_u+0.4M^*}\right)^c}}\mathrm{d}M,\end{aligned} \quad (31)$$

where M is the absolute magnitude, M^* is the characteristic magnitude, M_l is the lower boundary of the magnitudes and M_u is the upper boundary of the magnitudes. The two luminosities L_l and L_u are connected with the absolute magnitudes M_l and M_u through the following relation:

$$\frac{L_l}{L_\odot}=10^{0.4\left(M_\odot-M_u\right)},\frac{L_u}{L_\odot}=10^{0.4\left(M_\odot-M_l\right)} \quad (32)$$

where the indices *u* and *l* are inverted in the transformation from luminosity to absolute magnitude. The mean theoretical absolute magnitude, $\langle M\rangle$, can be evaluated as

$$\langle M\rangle=\frac{\int_{M_l}^{M_u}M\times\Psi\left(M;a,c,M^*,\Psi^*,M_l,M_u\right)\mathrm{d}M}{\int_{M_l}^{M_u}\Psi\left(a,M;c,M^*,\Psi^*,M_l,M_u\right)\mathrm{d}M}. \quad (33)$$

5. Astrophysical Applications

In this section, we review the adopted statistics and we apply the truncated NWPD to: the initial mass function for stars (IMF), which is often modeled by the lognormal distribution [20]; the LF for galaxies, which is usually modeled by the Schechter LF [14]; the photometric maximum for galaxies, which is modeled by the Schechter LF and the generalized gamma LF [21]; and the mean absolute magnitude for galaxies, which at the moment of writing has not yet been modelled by a probability distribution.

5.1. Statistics

The merit function χ^2 is computed according to the formula

$$\chi^2 = \sum_{i=1}^{n} \frac{(T_i - O_i)^2}{T_i}, \tag{34}$$

where n is the number of bins, T_i is the theoretical value, and O_i is the experimental value represented by the frequencies. The theoretical frequency distribution is given by

$$T_i = N \Delta x_i p(x), \tag{35}$$

where N is the number of elements of the sample, Δx_i is the magnitude of the size interval, and $p(x)$ is the PDF under examination. A reduced merit function χ^2_{red} is given by

$$\chi^2_{red} = \chi^2 / NF, \tag{36}$$

where $NF = n - k$ is the number of degrees of freedom, n is the number of bins, and k is the number of parameters. The goodness of the fit can be expressed by the probability Q, see equation 15.2.12 in [22], which involves the number of degrees of freedom and χ^2. According to [22] p. 658, the fit "may be acceptable" if $Q > 0.001$. The Akaike information criterion (AIC), see [23], is defined by

$$\mathrm{AIC} = 2k - 2\ln(L), \tag{37}$$

where L is the likelihood function and k the number of free parameters in the model. We assume a Gaussian distribution for the errors. Then the likelihood function can be derived from the χ^2 statistic $L \propto \exp\left(-\frac{\chi^2}{2}\right)$ where χ^2 has been computed by Equation (34)), see [24] [25]. Now the AIC becomes

$$\mathrm{AIC} = 2k + \chi^2. \tag{38}$$

The Kolmogorov-Smirnov test (K-S), see [26] [27] [28], does not require binning the data. The K-S test, as implemented by the FORTRAN subroutine KSONE in [22], finds the maximum distance, D, between the theoretical and the astronomical CDFs as well as the significance level P_{KS}, see Formulas (14.3.5) and (14.3.9) in [22]; if $P_{KS} \geq 0.1$, the goodness of the fit is believable.

5.2. The IMF for Stars

The *first* test is performed on NGC 2362 where the 271 stars have a range $1.47 M_{\odot} \geq M \geq 0.11 M_{\odot}$, see [29] and CDS catalog J/MNRAS/384/675/table 1. The *second* test is performed on the low-mass IMF in the young cluster NGC 6611, see [30] and CDS catalog J/MNRAS/392/1034. This massive cluster has an age of 2 - 3 Myr and contains masses from $1.5 M_{\odot} \geq M \geq 0.02 M_{\odot}$. Therefore the brown dwarfs (BD) region, $\approx 0.2 \mathcal{M}_{\odot}$ is covered. The *third* test is performed on the γ Velorum cluster where the 237 stars have a range $1.31 M_{\odot} \geq M \geq 0.15 M_{\odot}$, see [31] and CDS catalog J/A + A/589/A70/table 5. The *fourth* test is performed on the young cluster Berkeley 59 where the 420 stars have a range $2.24 M_{\odot} \geq M \geq 0.15 M_{\odot}$, see [32] and CDS catalog J/AJ/155/44/table 3. The results are presented in **Table 1** for the truncated NWPD with three parameters, where the last column reports whether the results are better compared to the Weibull distribution (Y) or worse (N).

As an example, the empirical PDF visualized through histograms as well as the theoretical PDF for NGC 2362 and NGC 6611 are reported in Figure 2 and in Figure 3 respectively.

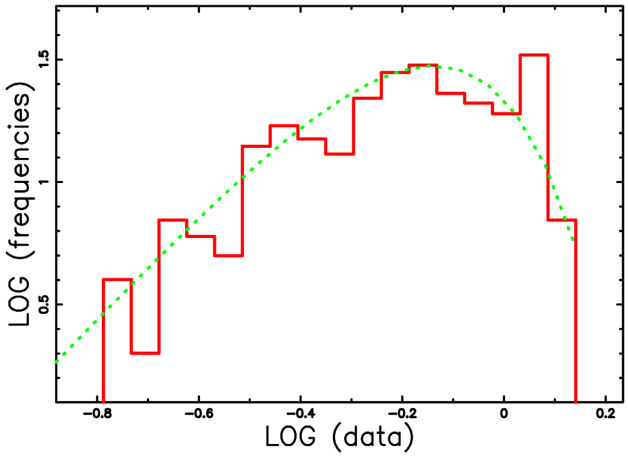

Figure 2. Empirical PDF of the mass distribution for NGC 2362 (271 stars) (red histogram) with a superposition of the truncated NWPD (green dotted line). Theoretical parameters as in Table 1.

Table 1. Numerical values of χ^2_{red}, AIC, probability Q, D, the maximum distance between theoretical and observed DF, and P_{KS}, significance level, in the K-S test of the truncated NWPD with three parameters for different mass distributions. The last column (W) indicates an AIC lower (Y) or higher (N) than that for the Weibull distribution with two parameters. The number of linear bins, n, is 20.

Cluster	parameters	AIC	χ^2_{red}	Q	D	P_{KS}	W
NGC 2362	$a=0.553$, $b=0.555$, $c=2.202$, $x_l=0.12$, $x_u=1.47$	41.5	2.1	0.007	0.046	0.576	N
NGC 6611	$a=5.414$, $b=2.569$, $c=1.011$, $x_l=0.019$, $x_u=1.46$	49.77	2.651	4.9×10^{-4}	0.059	0.45	N
γ Velorum	$a=3.626$, $b=0.863$, $c=0.745$, $x_l=0.158$, $x_u=1.317$	33.248	1.549	0.079	0.063	0.292	N
Berkeley 59	$a=1.234$, $b=0.417$, $c=1.143$, $x_l=0.16$, $x_u=2.24$	85.71	5.047	4.198×10^{-10}	0.122	6.35×10^{-6}	N

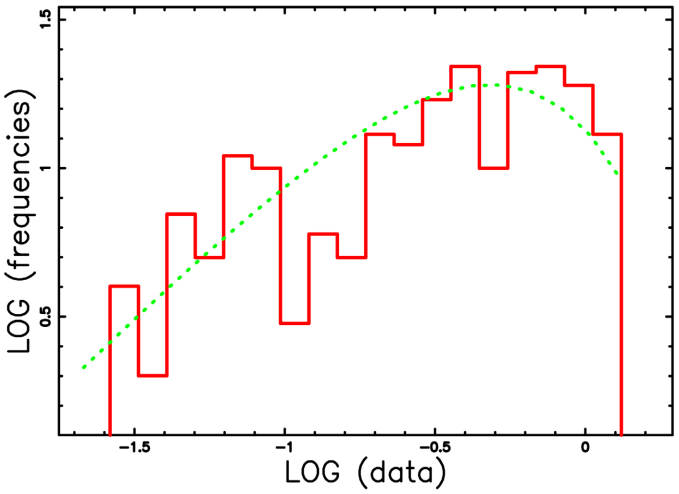

Figure 3. Empirical PDF of the mass distribution for young cluster NGC 6611 (207 stars) (red histogram) with a superposition of the truncated NWPD (green dotted line). Theoretical parameters as in **Table 1**.

5.3. The LF for Galaxies

We now perform the same test as in Section 5.3 in [33]. The Schechter function, the NWPD LF represented by Formula (29) and the data are reported in **Figure 4**, parameters as in **Table 2**.

A careful examination of **Table 2** reveals that the NWPD LF has a lower χ^2_{red} than for the Schechter LF. **Figure 5** reports the LF for QSO in the case $0.3 < z < 0.5$, see [34], with parameters as reported in **Table 3**.

5.4. The Photometric Maximum

In the pseudo-Euclidean universe, we introduce

$$z^2_{crit} = \frac{H_0^2 L^*}{4\pi f c_l^2}, \tag{39}$$

which allows defining the joint distribution in z (redshift) and f (flux) for NPWD LF as

$$\frac{\mathrm{d}N}{\mathrm{d}\Omega \mathrm{d}z \mathrm{d}f} = \frac{4z^2 c_l^5 \Psi^* a \left(\frac{z^2}{z^2_{crit}}\right)^c c\pi z^2_{crit} \mathrm{e}^{-a\left(\frac{z^2}{z^2_{crit}}\right)^c}}{H_0^5 L^*}, \tag{40}$$

where $\mathrm{d}\Omega$, $\mathrm{d}z$ and $\mathrm{d}f$ represent the differentials of the solid angle, the redshift, and the flux, respectively, L^* is the characteristic luminosity, c_l is the speed of light, and H_0 is the Hubble constant; see [33] for more details. The solution of the following non-linear equation determines a maximum at $z = z_{\max}$

$$-8z c_l^5 \Psi^* a \left(\frac{z^2}{z^2_{crit}}\right)^c c\pi z^2_{crit} \mathrm{e}^{-a\left(\frac{z^2}{z^2_{crit}}\right)^c} \left(\left(\frac{z^2}{z^2_{crit}}\right)^c ac - c - 1\right) = 0. \tag{41}$$

An analytical result can be obtained by computing a truncated multivariate

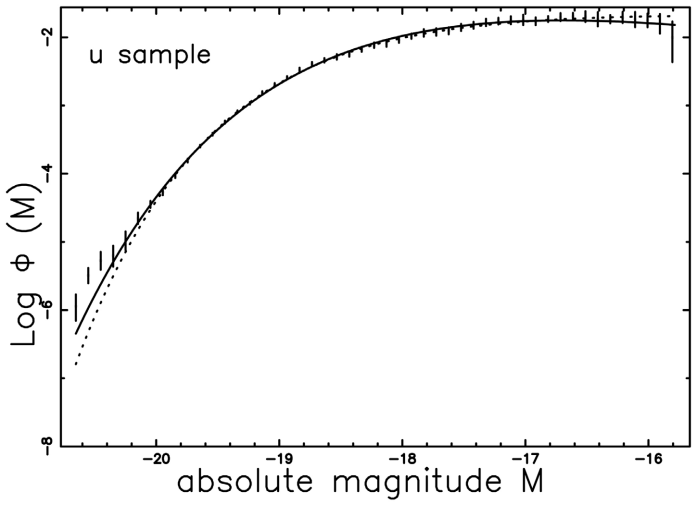

Figure 4. The LF data of SDSS (u^*) are represented with error bars. The continuous line fit represents the NWPD LF (29) and the dotted line represents the Schechter function.

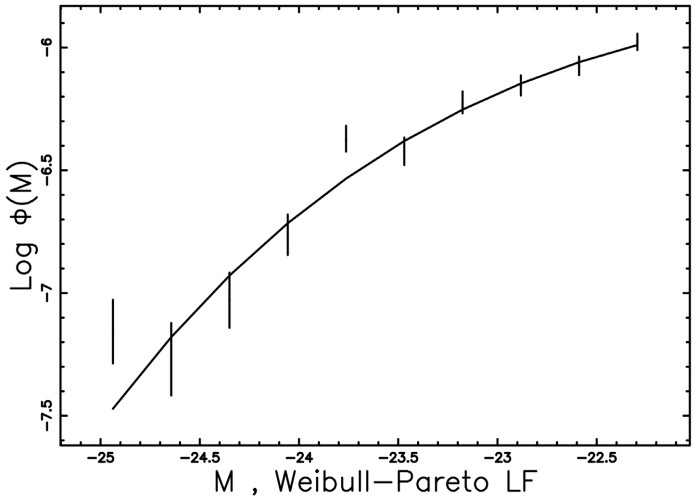

Figure 5. The observed LF for QSOs, empty stars with error bar, and the fit by the NWPD LF for z in $[0.3,0.5]$ and M in $[-24.93,-22]$. Parameters as in **Table 3**.

Table 2. Numerical values and χ^2_{red} of the LFs applied to SDSS Galaxies in the u^* band.

LF	parameters	χ^2_{red}
Schechter	$M^*=-17.92$, $\alpha=-0.9$, $\Phi^*=0.03/\mathrm{Mpc}^3$	0.689
NWPD	$M^*=-17.86$, $a=2.18$, $c=0.728$, $\Psi^*=0.0718/\mathrm{Mpc}^3$	0.651

Table 3. Parameters of the NWPD LF for QSOs in the range of redshift $[0.3,0.5]$ when $k=4$ and $n=10$.

M^*	Ψ^*	a	c	χ^2	χ^2_{red}	Q	AIC
−23.46	9.26×10^{-6}	3.52	0.471	10.08	1.68	0.121	18.08

Taylor series expansion of Equation (41), with respect to the variables z and a, to order n. As an example, when $z = 3 * z_{crit}$, $a = 1$ and $n = 2$, we have the following approximate equation which defines the photometric maximum as a function of a and b

$$\begin{aligned}&\frac{1}{H_0^5 L^*} Y^* 8\pi e^{2c\ln(3)-e^{2c\ln(3)}} c_l^5 c z_{crit}^2 \left(381^c acz_{crit} + 281^c c^2 z - 681^c c^2 z_{crit}\right.\\&-9e^{2c\ln(3)} acz_{crit} - 6e^{2c\ln(3)} c^2 z + 18e^{2c\ln(3)} c^2 z_{crit} - 381^c cz_{crit} - 3ae^{2c\ln(3)} z_{crit}\\&-3e^{2c\ln(3)} cz + 15e^{2c\ln(3)} cz_{crit} + 3acz_{crit} + 2c^2 z - 6c^2 z_{crit} + 3e^{2c\ln(3)} z_{crit}\\&\left.+3az_{crit} + 3cz - 9cz_{crit} + z - 3z_{crit}\right) = 0.\end{aligned} \quad (42)$$

Figure 6 reports the approximate solution to the third order ($z = 3 * z_{crit}$, $a = 1$, $n = 2$) of the photometric maximum which can be found selecting the positive solution of an algebraic equation of second degree.

Figure 7 reports a comparison of the truncated multivariate Taylor series and the numerical solution.

A numerical result is reported in **Figure 8** where we display the number of observed galaxies for the 2 MASS Redshift Survey (2 MRS) catalog at a given apparent magnitude and both the Schechter and the NWPD models for the number of galaxies as functions of the redshift. The theoretical parameters of the two curves in the above figure are chosen so as to minimize χ^2. One distribution (the full line) gives a better fit to the data at lower redshift than the other (the dashed line), while for the higher redshift, the opposite is true.

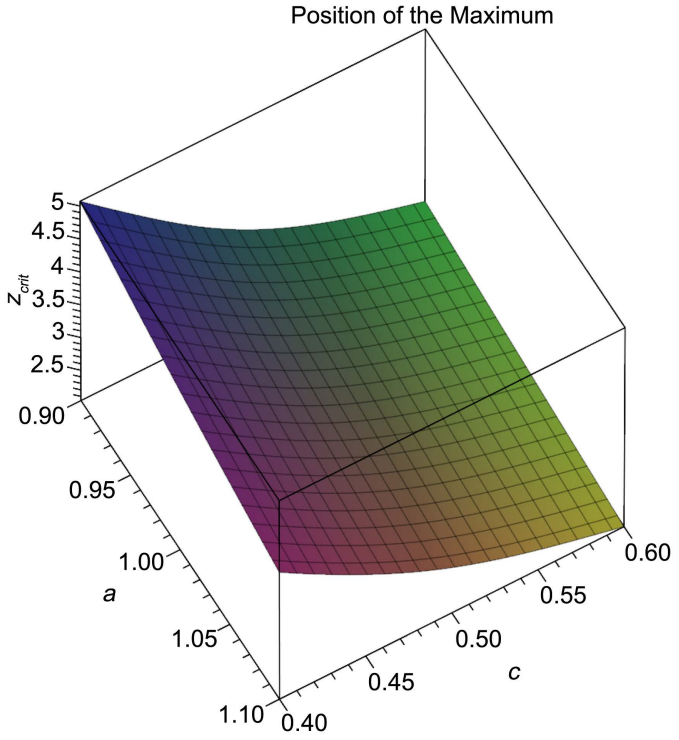

Figure 6. Approximate positive solution of the photometric maximum in units of z_{crit} when $z = 3 * z_{crit}$, $a = 1$ and $n = 3$ as a function of the parameters a and b.

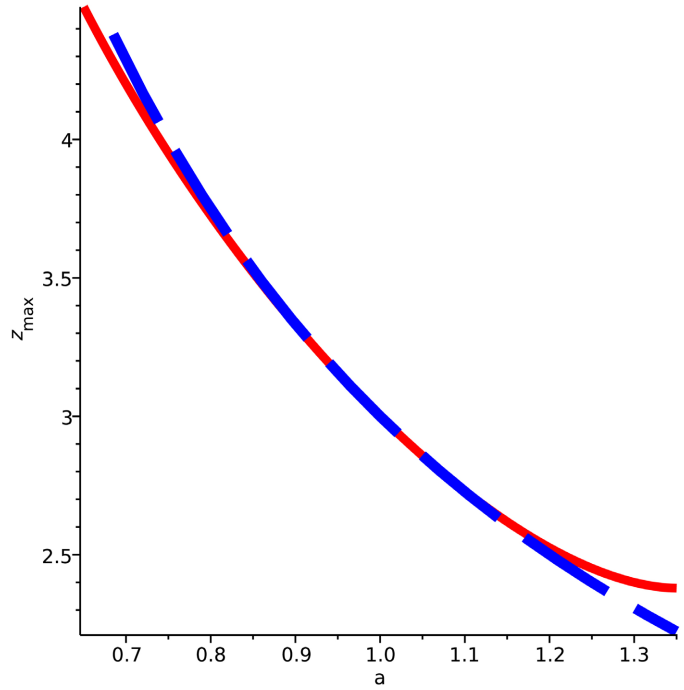

Figure 7. Approximate positive solution of the photometric maximum in units of z_{crit} ($z = 3 * z_{crit}$, $a = 1$, $n = 3$) as a function of the parameters a (blue dotted line) and numerical solution (red full line).

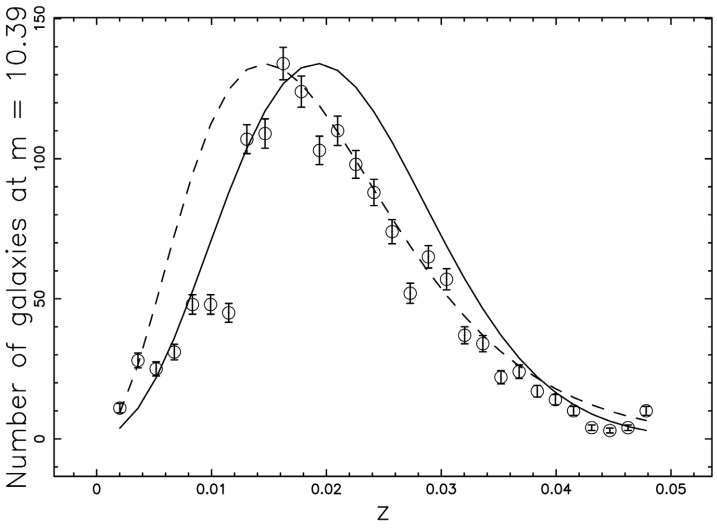

Figure 8. The galaxies of the 2 MRS with $10.31 \le m \le 10.47$ or $1164793 \frac{L_\odot}{\text{Mpc}^2} \le f \le 1346734 \frac{L_\odot}{\text{Mpc}^2}$ are organized in frequencies versus heliocentric redshift, (empty circles); the error bar is given by the square root of the frequency. The maximum frequency of observed galaxies is at $z = 0.017$. The full line is the theoretical curve generated by $\frac{dN}{d\Omega dz df}(z)$ as given by the application of the Schechter LF which is Equation (43) in [35] and the dashed line represents the NWPD LF which is Equation (40). The NWPD LF parameters are $a = 1.05$, $c = 1/2$, $M^* = -20.65$, $\chi^2 = 198$ for the Schechter LF and $\chi^2 = 420$ for the NWPD LF.

5.5. Mean Absolute Magnitude

We review the most important equations that allow modelling the mean absolute magnitude as a function of the redshift. The absolute magnitude is

$$M_L = m_L - 5\log_{10}\left(\frac{cz}{H_0}\right) - 25, \tag{43}$$

where $m_L = 11.75$ for the 2 MRS catalog.

The theoretical average absolute magnitude of the truncated NWPD LF, see Equation (33), can be compared with the observed average absolute magnitude of the 2 MRS as a function of the redshift. To fit the data, we assumed the following empirical dependence on the redshift for the characteristic magnitude of the truncated NWPD LF

$$M^* = -25.14 + 4\left(1 - \left(\frac{z - z_{\min}}{z_{\max} - z_{\min}}\right)^{0.7}\right), \tag{44}$$

where $z_{\min}$ and $z_{\max}$ are the minimum and the maximum value of the redshift in the considered catalog, in the case of the 2 MRS catalog $z_{\min} = 1.03\times10^{-4}$ and $z_{\max} = 4.49\times10^{-2}$. The lower bound in absolute magnitude is given by the minimum magnitude of the selected bin, the upper bound is given by Equation (43), the characteristic magnitude varies according to Equation (44) and Figure 9 shows a comparison between the theoretical and the observed absolute magnitude for the 2 MRS catalog.

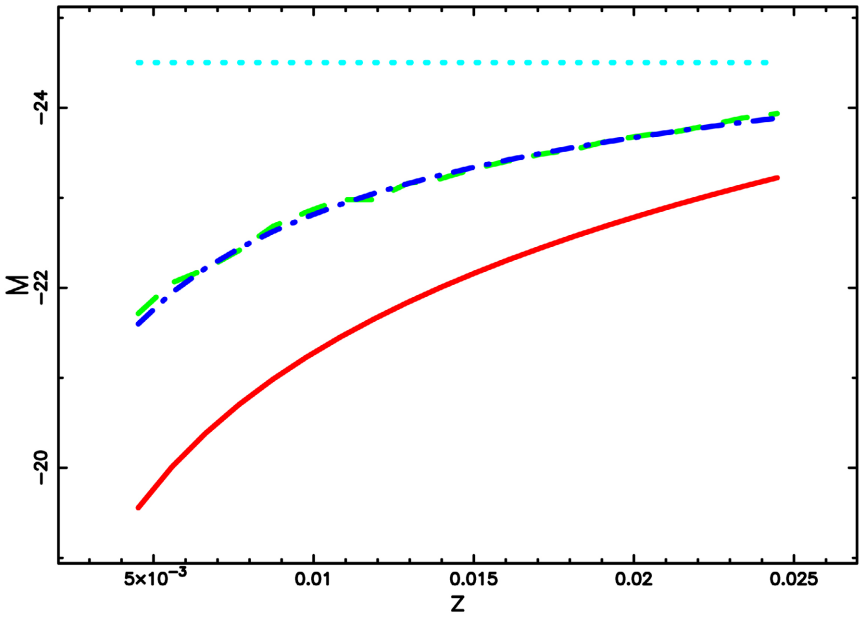

Figure 9. Average absolute magnitude of the galaxies belonging to the 2 MRS (green-dashed line), theoretical average absolute magnitude for the truncated NWPD LF (blue dash-dot-dash-dot line) as given by Equation (33) with $a = 1.1$ and $c = 1/2$, lower theoretical curve as represented by Equation (43) (red line) and minimum absolute magnitude observed (cyan dotted line).

6. Conclusions

The truncated Weibull-Pareto distribution. We derived the PDF, the DF, the average value, the rth moment, the median and an expression to generate random variates. The three parameters, a, b and c are derived by the MLE or by the method of moments for the truncated Weibull-Pareto distribution.

Quality of fits

The third parameter a of the NWPD adds flexibility to the usual Weibull distribution and as an example, Table 1 reports the parameters for four samples of stars, but due to Formula (4) the reduced χ^2 is not lower than those for the Weibull distribution.

Weibull—Pareto luminosity function

The NWPD LF in the absolute magnitude version is derived using the standard and the truncated DFs, see Formulas (29) and (31). The application to both the SDSS Galaxies and to the QSOs in the range of redshift $[0.3, 0.5]$ yields a lower reduced merit function than that from using the Schechter LF, see Table 2 and Figure 5.

Cosmological applications

The maximum in the number of galaxies for a given solid angle as a function of the redshift which is visible in the catalog of galaxies can be modeled with the NWPD LF, see Figure 8. The average absolute magnitude of the 2 MRS galaxies as a function of the redshift, can be theoretically modeled with the truncated NWPD LF, see Figure 9.

Conflicts of Interest

The author declares no conflicts of interest regarding the publication of this paper.

References

[1] Weibull, W. (1939) A Statistical Theory of Strengths of Materials. Vetenskaps Akademiens Handligar No. 151.

[2] Weibull, W. (1951) A Statistical Distribution Function of Wide Applicability. *Journal of Applied Mechanics*, **18**, 293-297. https://doi.org/10.1115/1.4010337

[3] Rinne, H. (2008) The Weibull Distribution: A Handbook. Chapman and Hall/CRC, London. https://doi.org/10.1201/9781420087444

[4] Nasiru, S. and Luguterah, A. (2015) The New Weibull-Pareto Distribution. *Pakistan Journal of Statistics and Operation Research*, **11**, 103-114. https://doi.org/10.18187/pjsor.v11i1.863

[5] Tahir, M.H., Cordeiro, G.M., Alzaatreh, A., Mansoor, M. and Zubair, M. (2016) A New Weibull-Pareto Distribution: Properties and Applications. *Communications in Statistics-Simulation and Computation*, **45**, 3548-3567. https://doi.org/10.1080/03610918.2014.948190

[6] Almetwally, E.M., Almongy, H.M., *et al.* (2019) Estimation Methods for the New Weibull-Pareto Distribution: Simulation and Application. *Journal of Data Science*, **17**, 610-630.

[7] Jeyadurga, P. and Balamurali, S. (2021) Multiple Deferred State Sampling Plan for Exponentiated New Weibull Pareto Distributed Mean Life Assurance. *Journal of Testing and Evaluation*, **49**, Article ID: 20200510. https://doi.org/10.1520/JTE20200510

[8] Mutair, A. and Karam, N.S. (2021) Stress-Strength Reliability for $P(T < X < Z)$ Using the New Weibull-Pareto Distribution. *Al-Qadisiyah Journal of Pure Science*, **26**, 39-51. https://doi.org/10.29350/qjps.2021.26.2.1259

[9] Shrahili, M., Al-Omari, A.I. and Alotaibi, N. (2021) Acceptance Sampling Plans from Life Tests Based on Percentiles of New Weibull-Pareto Distribution with Application to Breaking Stress of Carbon Fibers Data. *Processes*, **9**, Article No. 2041. https://doi.org/10.3390/pr9112041

[10] Afify, A.Z., Yousof, H.M., Butt, N.S. and Hamedani, G.G. (2016) The Transmuted Weibull-Pareto Distribution. *Pakistan Journal of Statistics*, **32**, 183-206.

[11] Tahir, A., Akhter, A.S., *et al.* (2018) Transmuted New Weibull-Pareto Distribution and Its Applications. *Applications and Applied Mathematics: An International Journal* (*AAM*), **13**, 30-46.

[12] Al-Omari, A., Al-khazaleh, A. and Alzoubi, L. (2020) A Generalization of the New-Weibull Pareto Distribution. *Revista Investigación Operacional*, **41**, 138-146.

[13] Damian, B., Jose, J., Samal, M.R., Moraux, E., Das, S.R. and Patra, S. (2021) Testing the Role of Environmental Effects on the Initial Mass Function of Low-Mass Stars. *Monthly Notices of the Royal Astronomical Society*, **504**, 2557-2576. https://doi.org/10.1093/mnras/stab194

[14] Schechter, P. (1976) An Analytic Expression for the Luminosity Function for Galaxies. *ApJ*, **203**, 297-306. https://doi.org/10.1086/154079

[15] Madgwick, D.S., Lahav, O., Baldry, I.K., Baugh, C.M., Bland-Hawthorn, J. and Bridges, T. (2002) The 2dF Galaxy Redshift Survey: Galaxy Luminosity Functions per Spectral Type. *MNRAS*, **333**, 133-144. https://doi.org/10.1046/j.1365-8711.2002.05393.x

[16] Blanton, M.R., Hogg, D.W., Bahcall, N.A., Brinkmann, J. and Britton, M. (2003) The Galaxy Luminosity Function and Luminosity Density at Redshift z = 0.1. *ApJ*, **592**, 819-838. https://doi.org/10.1086/375776

[17] Driver, S.P., Liske, J., Cross, N.J.G., De Propris, R. and Allen, P.D. (2005) The Millennium Galaxy Catalogue: The Space Density and Surface-Brightness Distribution(s) of Galaxies. *MNRAS*, **360**, 81-103. https://doi.org/10.1111/j.1365-2966.2005.08990.x

[18] Forbes, C., Evans, M., Hastings, N. and Peacock, B. (2011) Statistical Distributions. Fourth Edition, John Wiley & Sons, Hoboken. https://doi.org/10.1002/9780470627242

[19] Olver, F.W.J., Lozier, D.W., Boisvert, R.F. and Clark, C.W. (2010) NIST Handbook of Mathematical Functions. Cambridge University Press, Cambridge.

[20] Chabrier, G. (2003) Galactic Stellar and Substellar Initial Mass Function. *PASP*, **115**, 763-795. https://doi.org/10.1086/376392

[21] Zaninetti, L. (2014) A Near Infrared Test for Two Recent Luminosity Functions for Galaxies. *Revista Mexicana de Astronomia y Astrofisica*, **50**, 7-14.

[22] Press, W.H., Teukolsky, S.A., Vetterling, W.T. and Flannery, B.P. (1992) Numerical Recipes in FORTRAN. The Art of Scientific Computing. Cambridge University Press, Cambridge.

[23] Akaike, H. (1974) A New Look at the Statistical Model Identification. *IEEE Transactions on Automatic Control*, **19**, 716-723. https://doi.org/10.1109/TAC.1974.1100705

[24] Liddle, A.R. (2004) How Many Cosmological Parameters? *MNRAS*, **351**, L49-L53. https://doi.org/10.1111/j.1365-2966.2004.08033.x

[25] Godlowski, W. and Szydowski, M. (2005) Constraints on Dark Energy Models from Supernovae. In: Turatto, M., Benetti, S., Zampieri, L. and Shea, W., Eds., 1604-2004: *Supernovae as Cosmological Lighthouses*, Vol. 342 of Astronomical Society of the Pacific Conference Series, Astronomical Society of the Pacific, San Francisco, 508-516.

[26] Kolmogoroff, A. (1941) Confidence Limits for an Unknown Distribution Function. *The Annals of Mathematical Statistics*, **12**, 461-463. https://doi.org/10.1214/aoms/1177731684

[27] Smirnov, N. (1948) Table for Estimating the Goodness of Fit of Empirical Distributions. *The Annals of Mathematical Statistics*, **19**, 279-281. https://doi.org/10.1214/aoms/1177730256

[28] Massey Frank, J.J. (1951) The Kolmogorov-Smirnov Test for Goodness of Fit. *Journal of the American Statistical Association*, **46**, 68-78. https://doi.org/10.1080/01621459.1951.10500769

[29] Irwin, J., Hodgkin, S., Aigrain, S., Bouvier, J., Hebb, L., Irwin, M. and Moraux, E. (2008) The Monitor Project: Rotation of Low-Mass Stars in NGC 2362—Testing the Disc Regulation Paradigm at 5 Myr. *MNRAS*, **384**, 675-686. https://doi.org/10.1111/j.1365-2966.2007.12725.x

[30] Oliveira, J.M., Jeffries, R.D. and van Loon, J.T. (2009) The Low-Mass Initial Mass Function in the Young Cluster NGC 6611. *MNRAS*, **392**, 1034-1050. https://doi.org/10.1111/j.1365-2966.2008.14140.x

[31] Prisinzano, L., Damiani, F., *et al.* (2016) The Gaia-ESO Survey: Membership and Initial Mass Function of the γ Velorum Cluster. *A&A*, **589**, Article No. A70. https://doi.org/10.1051/0004-6361/201527875

[32] Panwar, N., Pandey, A.K., Samal, M.R., *et al.* (2018) Young Cluster Berkeley 59: Properties, Evolution, and Star Formation. *The Astronomical Journal*, **155**, Article No. 44. https://doi.org/10.3847/1538-3881/aa9f1b

[33] Zaninetti, L. (2021) New Probability Distributions in Astrophysics: V. The Truncated Weibull Distribution. *International Journal of Astronomy and Astrophysics*, **11**, 133-149. https://doi.org/10.4236/ijaa.2021.111008

[34] Zaninetti, L. (2017) A Left and Right Truncated Schechter Luminosity Function for Quasars. *Galaxies*, **5**, Article No. 25. https://doi.org/10.3390/galaxies5020025

[35] Zaninetti, L. (2019) The Truncated Lindley Distribution with Applications in Astrophysics. *Galaxies*, **7**, 61-78. https://doi.org/10.3390/galaxies7020061